Pinch-type instability experiments in magnetic Taylor-Couette flows

G. Rüdiger[1] and D.A. Shalybkov[1,2]

[1] Astrophysikalisches Institut Potsdam, An der Sternwarte 16, D-14482 Potsdam, Germany
[2] A.F. Ioffe Institute of Physics and Technology, 194021 St. Petersburg, Russia

E-mail: `gruediger@aip.de`

Abstract. The linear stability problem of MHD Taylor-Couette flows with toroidal magnetic fields and with resting outer cylinder is considered for very small magnetic Prandtl numbers. Except for radial profiles of $B_\phi(R) \propto 1/R$ (the current-free solution) the magnetic field destabilizes the flow. In particular, the most uniform field with $B_{\rm in} = B_{\rm out}$ has been considered. For weak fields the TC-flow is *stabilized* until for growing magnetic amplitude disturbances with $m = 1$ a dramatic destabilization of the flow starts. For high enough Hartmann numbers the toroidal field is always (pinch-)unstable independent of any details of the flow.
The electrical currents which are necessary for experiments in the laboratory must have amplitudes of a few kA for liquid sodium. The wider the gap of the container the weaker currents are necessary so that for wide-gap flows even experiments with gallium (Pm $\simeq 10^{-6}$) are possible. There are many fundamental applications of the Tayler (or pinch-type) instability in astrophysics.

1. Motivation

Taylor-Couette flows of electrically conducting fluid between rotating concentric cylinders are a classical problem of hydrodynamic and hydromagnetic stability theory. It is becoming increasingly clear that the stability of differential rotation combined with magnetic fields is also one of the key problems in MHD astrophysics. For uniform axial magnetic fields this phenomenon is called the magnetorotational instability (MRI). The Keplerian rotation of accretion disks with weak vertical magnetic fields becomes unstable, so that angular momentum is transported outward and gravitational energy is efficiently transformed into heat and radiation.

In contrast to these magnetorotational instabilities, in which the magnetic field acts as a catalyst, but not as a source of the energy, toroidal fields that are not current-free may become unstable more directly, by so-called current or pinch-type instabilities (Spruit 1999, Braithwaite and Nordlund 2006, Shalybkov 2006, Rüdiger et al. 2007). Because the source of energy is now the current rather than the differential rotation, these (nonaxisymmetric) instabilities can exist even without any differential rotation, provided only the current is large enough. The topic of this paper is how Tayler instabilities interact with differential rotation, and whether it might be possible to realize some of the resulting modes in laboratory experiments. The combination of Tayler instabilities and differential rotation may also be relevant to a broad range of astrophysical problems,

2. Equations

Vandakurov (1972) and Tayler (1973) found the necessary and sufficient condition

$$-\frac{\mathrm{d}}{\mathrm{d}R}(RB_\phi^2) > 0. \tag{1}$$

for the nonaxisymmetric stability of an ideal fluid at rest. Outwardly increasing fields are therefore unstable now. If this condition is violated, the most unstable mode has azimuthal wave number $m = 1$.

We focus on the limit of small magnetic Prandtl numbers appropriate for liquid metals, and calculate the rotation rates and electric currents that would be required to obtain some of these instabilities in liquid metal laboratory experiments.

Let $\mathbf{U}$ be the velocity, $\mathbf{B}$ the magnetic field, P the pressure, ν the kinematic viscosity, and η the magnetic diffusivity.

The basic state is $U_R = U_z = B_R = B_z = 0$ and

$$U_\phi = R\Omega = a_\Omega R + \frac{b_\Omega}{R}, \qquad B_\phi = a_B R + \frac{b_B}{R}, \tag{2}$$

where a_Ω, b_Ω, a_B and b_B are constants defined by

$$a_\Omega = \Omega_{\text{in}}\frac{\hat{\mu}_\Omega - \hat{\eta}^2}{1-\hat{\eta}^2}, \qquad b_\Omega = \Omega_{\text{in}}R_{\text{in}}^2\frac{1-\hat{\mu}_\Omega}{1-\hat{\eta}^2},$$
$$a_B = \frac{B_{\text{in}}}{R_{\text{in}}}\frac{\hat{\eta}(\hat{\mu}_B - \hat{\eta})}{1-\hat{\eta}^2}, \qquad b_B = B_{\text{in}}R_{\text{in}}\frac{1-\hat{\mu}_B\hat{\eta}}{1-\hat{\eta}^2}, \tag{3}$$

where

$$\hat{\eta} = \frac{R_{\text{in}}}{R_{\text{out}}}, \quad \hat{\mu}_\Omega = \frac{\Omega_{\text{out}}}{\Omega_{\text{in}}}, \quad \hat{\mu}_B = \frac{B_{\text{out}}}{B_{\text{in}}}. \tag{4}$$

R_{in} and R_{out} are the radii of the inner and outer cylinders, Ω_{in} and Ω_{out} are their rotation rates (we will in fact fix $\Omega_{\text{out}} = 0$ for all results presented here), and B_{in} and B_{out} are the azimuthal magnetic fields at the inner and outer cylinders. In particular, a field of the form b_B/R is generated by running an axial current only through the inner region $R < R_{\text{in}}$, whereas a field of the form $a_B R$ is generated by running an axial current through the entire region $R < R_{\text{out}}$, including the fluid. One of the aspects we will be interested in later on is how large these currents must be, and whether they could be generated in a laboratory experiment.

The dimensionless numbers of the problem are the magnetic Prandtl number Pm, the Hartmann number Ha, and the Reynolds number Re, given by

$$\text{Pm} = \frac{\nu}{\eta}, \qquad \text{Ha} = \frac{B_{\text{in}}R_0}{\sqrt{\mu_0\rho\nu\eta}}, \qquad \text{Re} = \frac{\Omega_{\text{in}}R_0^2}{\nu}, \tag{5}$$

where $R_0 = (R_{\text{in}}(R_{\text{out}} - R_{\text{in}}))^{1/2}$ is the unit of length.

Linearizing the equations the result is a system of first order equations. An appropriate set of ten boundary conditions is needed to solve it. For the velocity the boundary conditions are always no-slip, $u_R = u_\phi = u_z = 0$. For conducting walls the radial component of the field and the tangential components of the current must vanish, yielding $\mathrm{d}b_\phi/\mathrm{d}R + b_\phi/R = b_R = 0$. These boundary conditions are applied at both R_{in} and R_{out}.

We now focus attention on the limit of very small Pm, such as would apply for experiments involving liquid metals with conducting boundary conditions. Figure 1 shows results for various values of $\hat{\mu}_B$; a_B and b_B are the same sign for the values on the left, and the opposite sign for the values on the right. The profile that is closest to being current-free is $\hat{\mu}_B = 0$, and indeed we find there that even for $\mathrm{Ha} = 200$ there is no sign of any destabilizing influence of the field, for either axisymmetric or nonaxisymmetric perturbations.

For certain $\hat{\mu}_B$ the $m = 1$ mode should be unstable, while the $m = 0$ mode should be stable. The values $\hat{\mu}_B = 1$ and $\hat{\mu}_B = 2$ are examples of this situation. There is always a crossover point at which the most unstable mode changes from $m = 0$ to $m = 1$. Note also how for $\hat{\mu}_B = 1$, the critical Reynolds number increases for the $m = 0$ mode, before suddenly decreasing for the $m = 1$ mode We have the interesting situation therefore that weak fields initially stabilize the TC-flow, before stronger fields eventually destabilize it, via a nonaxisymmetric mode. Beyond $\mathrm{Ha} = 150$ the flow is unstable even for $\mathrm{Re} = 0$.

Except for the almost current-free profile $\hat{\mu}_B = 0$, all other values share this feature, that there is a critical Hartmann number beyond which the basic state is unstable even for $\mathrm{Re} = 0$. Let $\mathrm{Ha}^{(0)}$ and $\mathrm{Ha}^{(1)}$ denote these critical Hartmann numbers, for $m = 0$ and 1 respectively. For the profiles with the largest gradients both modes are unstable. Strikingly, in these cases $m = 0$ is always more unstable than $m = 1$, that is, $\mathrm{Ha}^{(0)} < \mathrm{Ha}^{(1)}$, see the plots for $\hat{\mu}_B = -1$ of Fig. 1.

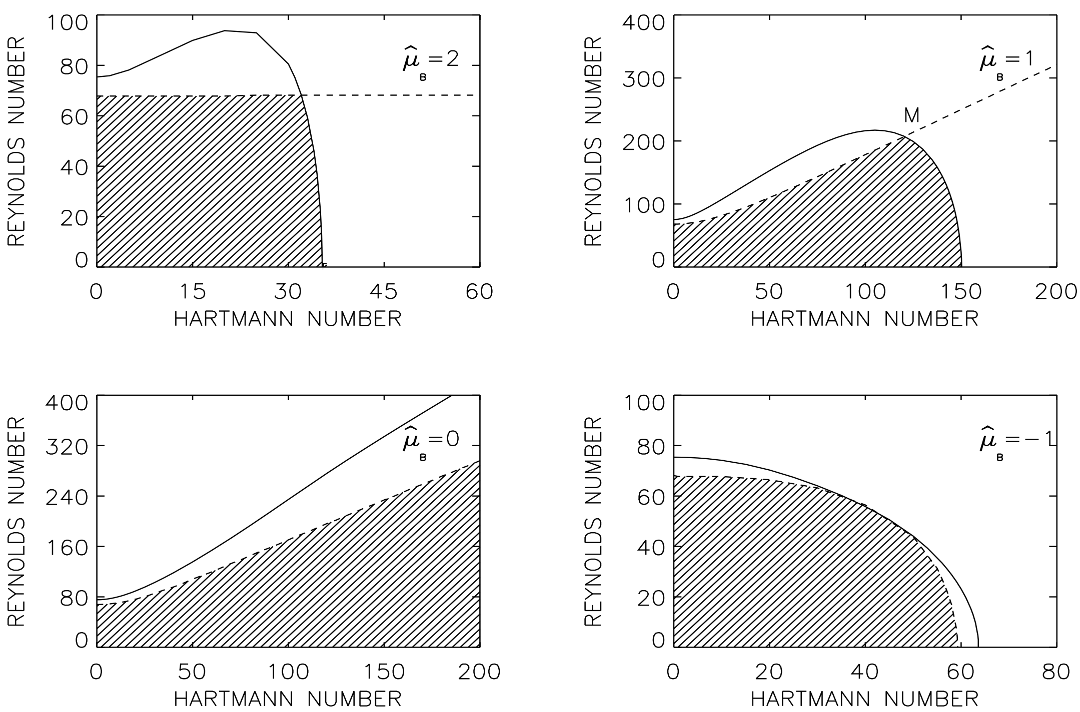

Figure 1. The marginal stability curves for $m = 0$ (dashed) and $m = 1$ (solid). $\mathrm{Pm}= 10^{-5}$, $\hat{\eta} = 0.5$, $\hat{\mu}_\Omega = 0$, and $\hat{\mu}_B$ as indicated. Note also how the critical Reynolds numbers are always of the same order of magnitude as the nonmagnetic result 68, which is easy to achieve in the laboratory.

3. Electric currents

Let I_{axis} be the axial current inside the inner cylinder and I_{fluid} the axial current through the fluid (i.e. between inner and outer cylinder). The toroidal field amplitudes at the inner and outer cylinders are then

$$B_{\mathrm{in}} = \frac{I_{\mathrm{axis}}}{5R_{\mathrm{in}}}, \qquad B_{\mathrm{out}} = \frac{(I_{\mathrm{axis}} + I_{\mathrm{fluid}})}{5R_{\mathrm{out}}}, \tag{6}$$

where R, B and I are measured in cm, Gauss and Ampere. Expressing $I_{\rm axis}$ and $I_{\rm fluid}$ in terms of our dimensionless parameters one finds

$$I_{\rm axis} = 5{\rm Ha}\ \frac{\hat{\eta}^{1/2}}{(1-\hat{\eta})^{1/2}}(\mu_0 \rho \nu \eta)^{1/2} \tag{7}$$

and

$$I_{\rm fluid} = \frac{\hat{\mu}_B - \hat{\eta}}{\hat{\eta}} I_{\rm axis} \tag{8}$$

in Ampere.

The results for the critical Hartmann numbers are applied to two different conducting liquid metals, sodium and gallium-indium-tin. Tables 1 and 2 give the values of the electric currents needed to reach the *lesser* of $\mathrm{Ha}^{(0)}$ and $\mathrm{Ha}^{(1)}$ for $\hat{\eta} = 0.5$, and for $\hat{\mu}_B$ ranging from -2 to 2 in each case. Note that for large $|\hat{\mu}_B|$, $\mathrm{Ha}^{(0)}$ scales as $1/\hat{\mu}_B$, and $I_{\rm fluid}$ approaches a constant value. The calculated currents are lower for fluids with smaller $\sqrt{\mu_0 \rho \nu \eta}$ (i.e. sodium is better than gallium).

In these Tables, the most interesting experiment, with the almost uniform field $\hat{\mu}_B = 1$ (see Fig. 1, top-right) is indicated in bold. For a container with a medium gap of $\hat{\eta} = 0.5$, parallel currents along the axis and through the fluid of 6.16 kA for sodium and 19.4 kA for gallium are necessary. Such sodium experiments should indeed be possible.

Table 1. Characteristic Hartmann numbers and electric currents for a wide gap container ($\hat{\eta} = 0.5$) with conducting walls, using sodium.

$\hat{\mu}_B$	$\mathrm{Ha}^{(0)}$	$\mathrm{Ha}^{(1)}$	$I_{\rm axis}$ [kA]	$I_{\rm fluid}$ [kA]
-2	19.8	24.8	0.807	-4.04
-1	59.3	63.7	2.42	-7.25
1	∞	**151**	**6.16**	**6.16**
2	∞	35.3	1.44	4.32

Table 2. The same as in Table 1 but for gallium-indium-tin.

$\hat{\mu}_B$	$\mathrm{Ha}^{(0)}$	$\mathrm{Ha}^{(1)}$	$I_{\rm axis}$ [kA]	$I_{\rm fluid}$ [kA]
-2	19.8	24.8	2.55	-12.7
-1	59.3	63.7	7.63	-22.9
1	∞	**151**	**19.4**	**19.4**
2	∞	35.3	4.54	13.6

[1] Braithwaite J and Nordlund Å 2006 *Astron. Astrophys.* **450** 1077
[2] Ruediger G, Hollerbach R, Schultz M and Elstner D 2007 *MNRAS* **377** 1481
[3] Shalybkov D 2006 *Phys. Rev.* E **73** 16302
[4] Spruit H 1999 *Astron Astrophys.* **349** 189
[5] Tayler R J 1973 *MNRAS* **161** 365
[6] Vandakurov Y V 1972 *Sov. Phys. A* bf16 265